

# The elastic behaviour and vibrational anharmonicity of molybdenum phosphate glasses

J. D. COMINS\*, J. E. MACDONALD, E. F. LAMBSON, G. A. SAUNDERS  
*School of Physics, University of Bath, Claverton Down, Bath BA2 7AY, UK*

A. J. ROWSELL, B. BRIDGE  
*Department of Physics, Brunel University, Uxbridge, Middlesex UB8 3PH, UK*

To examine the effects of vibrational anharmonicity on the long-wavelength phonon dynamics of a series of phosphate glasses, hydrostatic pressure and temperature dependences of ultrasonic wave velocities have been measured in molybdenum phosphate glasses  $(\text{MoO}_3)_x(\text{P}_2\text{O}_5)_{1-x}$  over the composition range 35 to 76 mol%  $\text{MoO}_3$ . Marked discontinuities occur in the variations of elastic constants with composition, indicating distinct differences in the nature of the structure and bonding in the glasses as a function of composition. The pressure derivatives of the elastic constants are found to be positive and the temperature derivatives negative. Both the longitudinal ( $\gamma_L$ ) and shear ( $\gamma_S$ ) mode Grüneisen parameters are positive, showing that application of hydrostatic pressure produces an increase in the long-wavelength acoustic phonon mode frequencies. The temperature dependences of both longitudinal and shear acoustic phonon velocities are found to be markedly anomalous in that they continue to increase substantially as the temperature is reduced below about 100 K. The low-temperature elastic constant data are compatible with the interaction of the phonons with two-level systems, and provide direct evidence for such systems in phosphate glasses.

## 1. Introduction

The molybdenum phosphate ( $\text{MoO}_3\text{-P}_2\text{O}_5$ ) glass system is stable over an unusually wide range (0 to ~83 wt%  $\text{MoO}_3$ ) of compositions and yet exhibits marked discontinuities in physical properties within this range [1].

To study the acoustic mode vibrational anharmonicity across this composition range, measurements have been made of the hydrostatic pressure dependences of ultrasonic wave velocities. The higher-order elasticity of glasses has been found to fall into two classes of behaviour [2, 3]. On the one hand vitreous silica and silica-based glasses have negative pressure derivatives of the bulk ( $B$ ) and shear ( $\mu$ ) moduli [4, 5]. On the other hand the pressure derivatives of  $B$  and  $\mu$  for many diverse types of glass are positive: the long-wavelength acoustic modes stiffen with pressure in accord with normally expected physical behaviour [2, 3, 6]. In the only previously reported study of the effect of pressure on the elastic properties of a phosphate glass, intermediate behaviour was found: the long-wavelength shear modes softened while the longitudinal modes stiffened when hydrostatic pressure was applied [7].

The hydrostatic pressure dependences of the ultrasonic wave velocities provide knowledge of the long-wavelength acoustic mode Grüneisen parameters  $\gamma_L$  and  $\gamma_S$ . Previously the mean parameter  $\gamma_{cl}$  has been

shown to be quite well correlated with the thermal expansion coefficient  $\alpha$  for a number of glass systems [6]. Accordingly, as part of this study of phonon anharmonicity, the closeness of the fit to this correlation of the properties of the molybdenum phosphate glasses has been inspected.

The temperature dependences of the second-order elastic stiffnesses are also expected to be determined by phonon anharmonicity. Therefore the elastic constants  $C_{ij}$  have been measured as a function of temperature between 4 and 300 K. Marked compositional effects on  $(\partial C_{ij}/\partial T)_{p=0,T}$  have been observed which can be correlated with the anharmonicity of phonon modes as determined from the high-pressure studies. Strong, anomalous increases in  $(\partial C_{ij}/\partial T)_{p=0,T}$  have been found at temperatures below about 100 K which can be associated with interactions in two-well systems.

Previous work [1] on this series of glasses has indicated the presence of structural groupings similar to those which occur as crystalline phases, namely  $\text{MoO}_2(\text{PO}_3)_2$  (metaphosphate),  $(\text{MoO}_2)_2\text{P}_2\text{O}_7$  (pyrophosphate) and  $\text{MoOPO}_4$  (orthophosphate) together with the end-number oxides  $\text{MoO}_3$  and  $\text{P}_2\text{O}_5$ . The concentrations of these component structural groupings vary considerably over the composition range. In particular, sharp concentration maxima were observed for the metaphosphate and pyrophosphate groupings

\*On sabbatical leave from Department of Physics, University of the Witwatersrand, Johannesburg 2001, South Africa.

TABLE I Crystalline groupings

Structural grouping	Associated smallest closed "ring"	$N_b$	$\bar{N}_c$	Molybdenum valency
$P_2O_5$	$P_6O_6$ or $P_{10}O_{10}$	6	1	—
$MoO_2(PO_3)_2$	$MoP_2O_3$	12	2	6
$(MoO_2)_2P_2O_7$	$Mo_2P_2O_4$	18	2.5	6
$MoOPO_4$	$Mo_2P_2O_4$	10	3	5
$MoO_3$	$Mo_2O_2$	5	3	6

at about 50 and 66 mol %  $MoO_3$  content, respectively. The changing proportions of the structural groupings comply with variations of the ratio of  $Mo^{5+}$  to  $Mo^{6+}$ . This ratio has a maximum value near 50 mol %  $MoO_3$  content and is associated with a reduction of  $Mo^{6+}$  to  $Mo^{5+}$ , and leads to discontinuities in the elastic moduli and other physical properties near 50 and 66 mol %  $MoO_3$ . A model based on the average atomic ring diameter, being determined by the dominant structural grouping appropriate to the composition range, can account in a qualitative manner for these compositional effects [1]. Tables I and II incorporate conclusions extracted from the work of Bridge and Patel [1] as an aid to the discussion. We note the existence of five structural groupings with their associated smallest ring type and other pertinent quantities:  $N_b$  (the number of network bonds per formula unit),  $\bar{N}_c$  (the mean crosslink density per cation) and the molybdenum valency. In forming glasses the presence of more than one structural grouping and the structural constraints imposed by the glass network lead to an average ring size  $s$  in terms of cations and anions and an average crosslink density  $\bar{n}_c$  per cation. In essence the model associates progressively smaller rings with increased elastic stiffness, and vice versa.

The central aim of the present work has been to answer the question: what influence does the changing concentration of component structural groupings across the glass composition range have on the vibrational anharmonicity of long-wavelength acoustic phonons?

## 2. Sample preparation, characterization and experimental techniques

The molybdenum phosphate glasses were prepared from dry mixtures of anhydrous  $MoO_3$  and  $P_2O_5$  mixed together in alumina crucibles and placed in a furnace initially held at 300°C below melt temperature. The temperature was then raised to an appropriate value between 900 and 1200°C and equilibrated for 20 min with frequent stirring to promote homogeneity. The melts were cast into stainless steel moulds maintained at the desired glass annealing temperature.

The density ( $\rho$ ) of each composition was taken from

TABLE II Glass structure

$MoO_3$ (%)	Structural groupings present	$s$	$\bar{n}_c$
26	$P_2O_5$ , $MoO_2(PO_3)_2$ , $MoOPO_4$	9.8	1.5
50	$MoO_2(PO_3)_2$ , $MoOPO_4$	6.9	~ 2.5
66	$(MoO_2)_2P_2O_7$ , $MoOPO_4$	9	2.5
80	$MoO_3$ , $(MoO_2)_2P_2O_7$	6.4	2.4

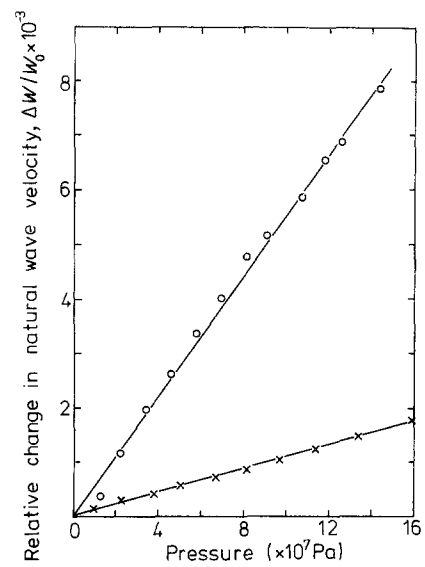


Figure 1 The dependence of relative natural velocity changes of 10 MHz ultrasonic waves upon applied hydrostatic pressure for a glass of composition 35 mol %  $MoO_3$ : (O) L, (x) S.

data from Patel [8] for molybdenum phosphate glasses; similar density results were obtained by Kierkegaard *et al.* [9]. Atomic absorption analysis was used to determine the  $MoO_3$  content and electron spin resonance studies provided the proportion of  $Mo^{5+}$  (paramagnetic) to  $Mo^{6+}$  (diamagnetic) species. Samples were prepared for ultrasonic studies with parallel faces using standard cutting and polishing techniques.

The velocities of longitudinal ( $v_L$ ) and shear ( $v_S$ ) ultrasonic waves in the glasses were obtained by using the pulse-echo-overlap technique. Ultrasonic pulses of frequency 10 MHz were generated and received by X- and Y-cut quartz transducers.

The hydrostatic pressure derivatives of the ultrasonic wave transit times were measured using a piston and cylinder high-pressure apparatus with castor oil as the pressure medium. The change in electrical resistivity of a manganin coil inside the pressure chamber was used to measure the hydrostatic pressure.

Fig. 1 illustrates a typical data set for the relative change induced by hydrostatic pressure in natural velocity, in this case for a glass of composition 35 mol %  $MoO_3$ . The pressure-induced changes in pulse echo overlap were expressed as the relative change of natural velocity ( $1/W_0$ ) ( $\Delta W/\Delta P$ ) where  $W_0$  is the natural wave velocity at atmospheric pressure and  $W$  is that at pressure  $P$ ; this procedure avoids the need to calculate sample dimensions under stress [10]. This quantity was found to be linear to  $1.6 \times 10^8$  Pa ( $= 1.6$  kbar) for both longitudinal and shear modes under hydrostatic pressure for all the samples tested (Fig. 1). The pressure derivatives of the elastic moduli

$$\left(\frac{\partial C_{ij}}{\partial P}\right)_{P=0} = \frac{C_{ij}}{3B} + 2C_{ij} \left[ \left(\frac{1}{W_0}\right) \frac{\Delta W}{\Delta P} \right]$$

allow the determination of

$$\begin{aligned} \left(\frac{dB}{dP}\right)_{P=0} &= \left(\frac{dC_{11}}{dP}\right) - \frac{4}{3} \left(\frac{dC_{44}}{dP}\right)_{P=0} \\ &= -\frac{C_{111} + 6C_{112} + 2C_{123}}{9B} \end{aligned}$$

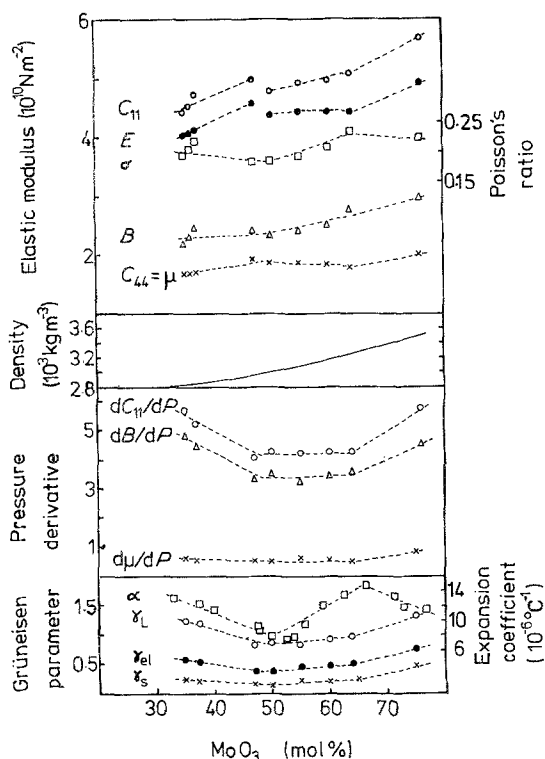


Figure 2 The elastic properties, hydrostatic pressure derivatives of the elastic stiffnesses, acoustic mode Grüneisen parameters at the long-wavelength limit, density and thermal expansion of molybdenum phosphate glasses as a function of MoO<sub>3</sub> content.

and

$$\begin{aligned} \left(\frac{d\mu}{dP}\right)_{P=0} &= \left(\frac{dC_{44}}{dP}\right)_{P=0} \\ &= -\frac{(6C_{11} - 6C_{44} + C_{111} - C_{123})}{6B} \end{aligned}$$

The values of  $(dC_{11}/dP)_{P=0}$ ,  $(dB/dP)_{P=0}$  and  $(\partial\mu/\partial P)_{P=0}$  are shown in Fig. 2. Each of these pressure derivatives is positive: these glasses stiffen under pressure.

The low-temperature dependences of the elastic constants were measured using a helium cryostat. On reaching 4.2 K, the sample was rewarmed and again measurements were carried out up to approximately 70 K. Excellent agreement was observed between cooling and warming runs.

### 3. Results and discussion

#### 3.1. The properties of molybdenum phosphate glasses at room temperature

Compositional trends in a number of physical properties are presented in Fig. 2 as a function of MoO<sub>3</sub> content for our suite of molybdenum phosphate

glasses. While the density depends monotonically on composition, other properties display discontinuities at about 50 and 64 mol % MoO<sub>3</sub>. These findings are in accord with those of Bridge and Patel [1], small numerical differences occurring between the results obtained on the two sets of glasses. Elastic moduli for the present samples containing more than about 64 mol % (the composition range in which the elastic properties are controlled by the (MoO<sub>2</sub>)<sub>2</sub>P<sub>2</sub>O<sub>7</sub> and MoO<sub>3</sub> grouping involving Mo<sup>6+</sup> [1], agree closely with those measured previously. The Mo<sup>5+</sup> content is a measure of the proportion of the MoOPO<sub>4</sub> structural grouping whose influence is to reduce the average ring size (Tables I and II) and increase elastic stiffnesses. Indeed, the magnitude of the discontinuity at about 50 mol % MoO<sub>3</sub> is largely controlled by the Mo<sup>5+</sup> content which has a sharp maximum at this concentration. In the present samples the [Mo<sup>5+</sup>/Mo(total)] ratios are somewhat smaller than those found in the samples of Bridge and Patel [1]. Hence our samples will tend to have a larger average ring size in the lower concentration range. Thus smaller values of the elastic moduli and a partial suppression of the discontinuity near 50 mol % MoO<sub>3</sub> can be expected – and are observed. The pressure derivatives display discontinuities at the same MoO<sub>3</sub> concentrations (~ 50 mol % and 64 mol %) as found for the elastic stiffnesses themselves (Fig. 2): the same structural and bonding influences must be operative in both the second- and third-order elastic behaviour.

Table III compares results for a selected molybdenum phosphate glass with those of other amorphous materials and also illustrates the fact that amorphous materials may be divided into two classes according to their elastic behaviour under pressure: those whose  $\partial B/\partial P$  and  $\partial\mu/\partial P$  are negative and positive, respectively. In this respect the phosphate glasses are interesting in that while  $\partial B/\partial P$  is quite large and positive,  $\partial\mu/\partial P$  is close to the transitional value of zero. The molybdenum phosphate glasses have a small but positive  $\partial\mu/\partial P$ , whereas in amorphous (Fe<sub>2</sub>O<sub>3</sub>)<sub>0.38</sub>(P<sub>2</sub>O<sub>5</sub>)<sub>0.62</sub> this quantity is slightly negative [7]. Bending vibrations of the individual bridging oxygen ions corresponding to transverse motion against small force constants are responsible for the negative pressure derivatives in silica-based glasses [12]. The near-zero  $\partial\mu/\partial P$  implies that such bending vibrations are largely but not entirely absent from the vibrational spectrum of phosphate glasses.

Physical properties which depend upon the thermal motion of the atoms are greatly influenced by vibrational anharmonicity, especially at higher temperatures. The higher-order elastic constants are

TABLE III Comparison of properties of molybdenum phosphate glasses with other amorphous materials at room temperature

Property	MoO <sub>3</sub> -P <sub>2</sub> O <sub>5</sub> glasses	(Fe <sub>2</sub> O <sub>3</sub> ) <sub>0.38</sub> (P <sub>2</sub> O <sub>5</sub> ) <sub>0.62</sub> [7]	Amorphous arsenic [2]	Amorphous As <sub>2</sub> S <sub>3</sub> [4]	Pd <sub>40</sub> Ni <sub>40</sub> P <sub>20</sub> (metglas) [11]	Pyrex [5]	Fused silica [5]
$(\partial B/\partial P)_{P=0}$	3.24 to 4.82	+ 4.73	+ 6.42	+ 6.52	+ 6.4	- 4.72	- 6.3
$(\partial\mu/\partial P)_{P=0}$	0.50 to 0.88	- 0.16	+ 1.73	+ 1.87	+ 1.8	- 2.39	- 4.1
$\gamma_L$	0.81 to 1.34	+ 1.1	+ 2.34	+ 2.61	+ 2.34	- 1.74	- 2.8
$\gamma_s$	0.15 to 0.48	- 0.3	+ 1.45	+ 2.49	+ 1.45	- 1.50	- 2.36
$\gamma_{el}$	0.38 to 0.77	+ 0.7	+ 1.75	+ 2.53	+ 1.75	- 1.58	- 2.5
$\alpha$ (10 <sup>-6</sup> °C <sup>-1</sup> )	7.5 to 14	-	+ 8 to + 10.3	+ 22.4	-	+ 3.2	+ 0.45

prerequisite for a quantitative understanding of the role played by long-wavelength acoustic modes in properties dominated by anharmonicity, such as the thermal expansion. A quantitative assessment of the anharmonicity of these particular modes is given by the appropriate Grüneisen parameters which express the volume (or strain) dependence of normal mode frequencies  $\omega_i$  by

$$\gamma_i = -d(\ln \omega_i)/d(\ln V)$$

and allow the effect of hydrostatic pressure on the  $\omega_i$  to be quantified. In an isotropic glass there are two components of the Grüneisen parameter for acoustic modes at the long-wavelength limit given by [6]

$$\begin{aligned} \gamma_L &= -B \left[ 3 - \left( \frac{2C_{12}}{B} \right) - 3 \left( \frac{\partial B}{\partial P} \right) \right. \\ &\quad \left. - 4 \left( \frac{\partial \mu}{\partial P} \right) \right] / 6C_{11} \\ \gamma_S &= - \left[ 2\mu - 3B \left( \frac{\partial \mu}{\partial P} \right) - 1.5B \right. \\ &\quad \left. + 1.5(C_{11} - 2C_{44}) \right] / 6\mu \end{aligned}$$

The mean long-wavelength acoustic mode Grüneisen parameter  $\gamma_{el}$  is given by

$$\gamma_{el} = (\gamma_L + 2\gamma_S)/3$$

$\gamma_L$ ,  $\gamma_S$  and  $\gamma_{el}$  have been obtained using these equations from the experimental data for the elastic constants and their pressure derivatives. The results are plotted as a function of glass composition in Fig. 2.

Besides determining the behaviour of a solid under pressure, vibrational anharmonicity is responsible for thermal expansion. Experimentally an average thermal Grüneisen parameter  $\gamma^{th}$  can be evaluated from

$$\gamma^{th} = 3\alpha V B_S / C_P = 3\alpha V B_T / C_V = \sum_i C_i \gamma_i / \sum_i C_i$$

where  $C_i$  is the contribution of mode  $i$  to the specific heat ( $C_V = \sum_i C_i$ ). We expect long-wavelength acoustic modes to make a substantial contribution to the collective summations  $\sum_i$  over the modes and thus anticipate a correlation between the room-temperature thermal expansion and  $\gamma_{el}$ . This is indeed observed (Fig. 2).

### 3.2. General correlation between thermal expansions and Grüneisen parameters for glasses

Both the long-wavelength acoustic mode Grüneisen parameters  $\gamma_S$  and  $\gamma_L$  are positive for the molybdenum phosphate glasses: the energies of both types of acoustic mode increase in the normal way under volumetric strain (in contrast to the behaviour of silica (Table III)). For a number of glasses there is a correlation [6] between the mean long-wavelength acoustic mode Grüneisen parameter  $\gamma_{el}$  and the thermal expansion coefficient  $\alpha$ . The rectangular box in Fig. 3 incorporates the  $\gamma_{el}$  data obtained here together with the thermal expansion results obtained [8] on another set of molybdenum phosphate glasses whose compositions

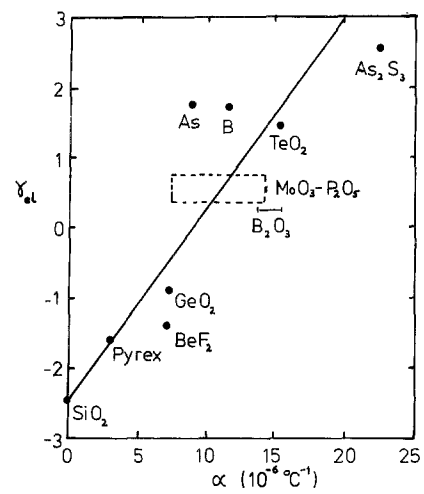


Figure 3 To show how the molybdenum phosphate glasses fit the correlation found [6] between the mean long-wavelength acoustic mode Grüneisen parameter and the linear coefficient  $\alpha$  of thermal expansion for glasses.

differ somewhat – precluding an exact comparison. However, as already stated, at higher  $\text{MoO}_3$  compositions the present elastic stiffnesses agree well with those obtained on the other glass set by Bridge and Patel [1]. Although the absolute values at lower  $\text{MoO}_3$  concentrations differ slightly, behavioural trends are reproduced. Hence the rectangular box in Fig. 3 does provide a useful assessment of the place occupied by phosphate glasses in the overall pattern of anharmonic vibrational behaviour of glasses. In general the observed correlation implies that the anharmonicities of long-wavelength acoustic phonons provide important contributions to the collective summations over the vibrational states which yield the thermal Grüneisen parameter  $\gamma^{th}$ . However, the detailed behaviour of the thermal expansion coefficient  $\alpha$  for the glasses containing  $\text{MoO}_3$  in excess of 64 mol % does not reflect the increase in  $\gamma_{el}$  found across this composition range, so that structure and bonding influences play a role in the properties determined by vibrational anharmonicity.

### 3.3. An equation of state for molybdenum phosphate glasses

The use of an equation of state permits an estimation of the compression of a material at very high pressures from a knowledge of the bulk modulus and its hydrostatic pressure derivative. This procedure has been carried out using the Murnaghan [13] equation of state

$$\ln \left( \frac{V}{V_0} \right) = - \frac{1}{B_0} \ln \left[ B_0' \left( \frac{P}{B_0} \right) + 1 \right]$$

which assumes that the bulk modulus depends linearly on pressure:

$$\begin{aligned} B(P) &= -V \left( \frac{\partial P}{\partial V} \right)_T = B_0 + P \left( \frac{\partial B}{\partial P} \right)_{P=0,T} \\ &= B_0 + P B_0' \end{aligned}$$

In Fig. 4 the results are plotted for the range of molybdenum phosphate glasses. Here we have used the adiabatic bulk modulus  $B_0^S$  rather than the isothermal

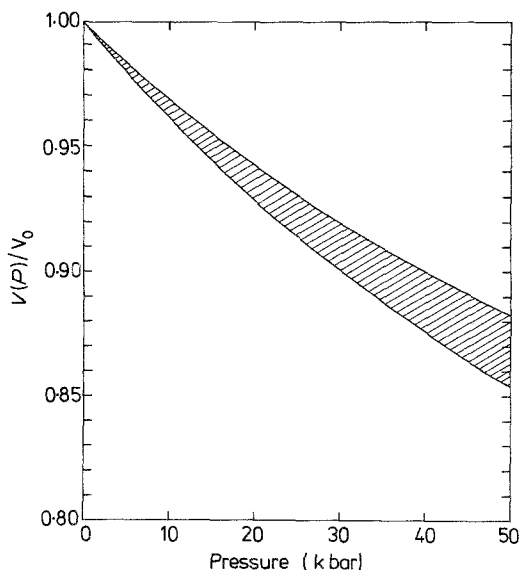
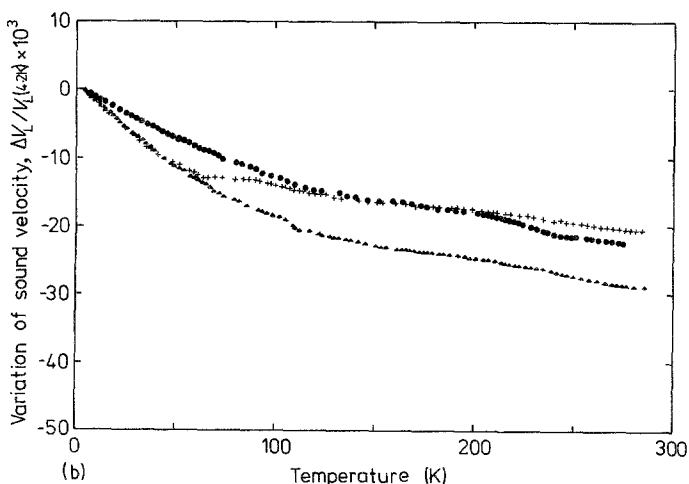
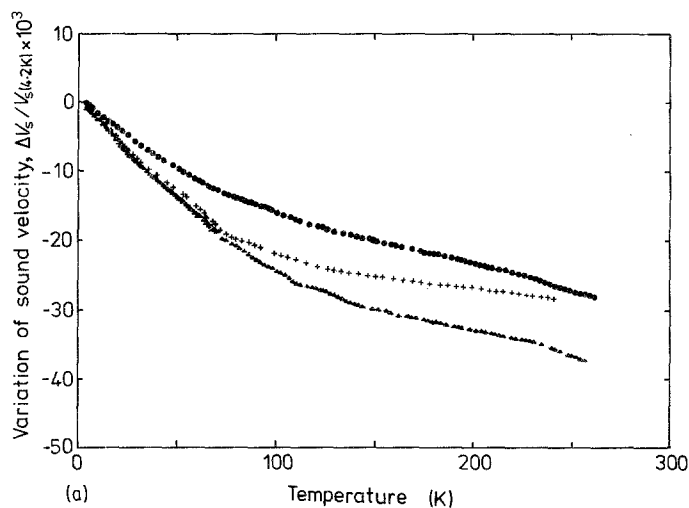


Figure 4 The compression of molybdenum phosphate glasses calculated on the basis of the Murnaghan equation of state [13]. The variation of compression with composition is represented by the hatched region. 1 kBar =  $10^8$  Pa.

quantity  $B_0^T$ . These are related by

$$B_0^T = B_0^S / (1 + \gamma^{\text{th}} \alpha T)$$

Using as an estimate of  $\gamma^{\text{th}}$  the mean long-wavelength acoustic parameter  $\gamma_{\text{el}}$  and an appropriate value of  $\alpha$  from Fig. 2, the fractional error in  $B_0^T$  is about 0.2% for the range of glasses. This introduces a discrepancy in  $B(P)$  which is very small in comparison to the variation shown between the glasses.



### 3.4. Temperature dependences of the elastic stiffnesses of molybdenum phosphate glasses

Figs 5a and b show the variation of  $\Delta v_L/v_L$  (4.2 K) and the corresponding plot for the shear-mode velocity as a function of temperature for different compositions. In Figs 6a and b we show the temperature dependences of the elastic constants suitably corrected for thermal expansion. The results are conveniently separated into two temperature ranges: (a) below about 130 K, where the presence of structural relaxation processes attributed to two-level systems is responsible for the observed increases in acoustic mode velocity and elastic constants, and (b) above about 130 K where anharmonic effects, the central concern of this particular investigation, are observed.

The results in region (a) show that both acoustic modes couple to the two-level systems and complement previous studies of the velocity [8] and attenuation [14] of the longitudinal mode only. To assess the magnitude of increased stiffness due to this effect, the constant values to be expected from the anharmonicity of the vibrational mode have been calculated on the basis of the quasi-harmonic approximation. This has been carried out on the assumption that all the vibrational modes have the same temperature-dependent Grüneisen parameter  $\gamma$  ( $= \bar{\gamma}_{\text{el}}(T)$ ), when the adiabatic stiffness moduli for longitudinal and transverse waves are given [15] respectively by

$$C_L = C_L^0 + \frac{1}{V} \left\{ -\gamma^2 - \gamma \left[ \left( \frac{\partial C_L}{\partial P} \right)_T - \frac{C_L}{3B} \right] \right\} U$$

Figure 5 The temperature dependences of velocities of (a) shear and (b) longitudinal wave velocities of 10 MHz ultrasonic waves propagated in molybdenum phosphate glasses. MoO<sub>3</sub> content (▲) 37, (+) 50, (●) 64 mol %.

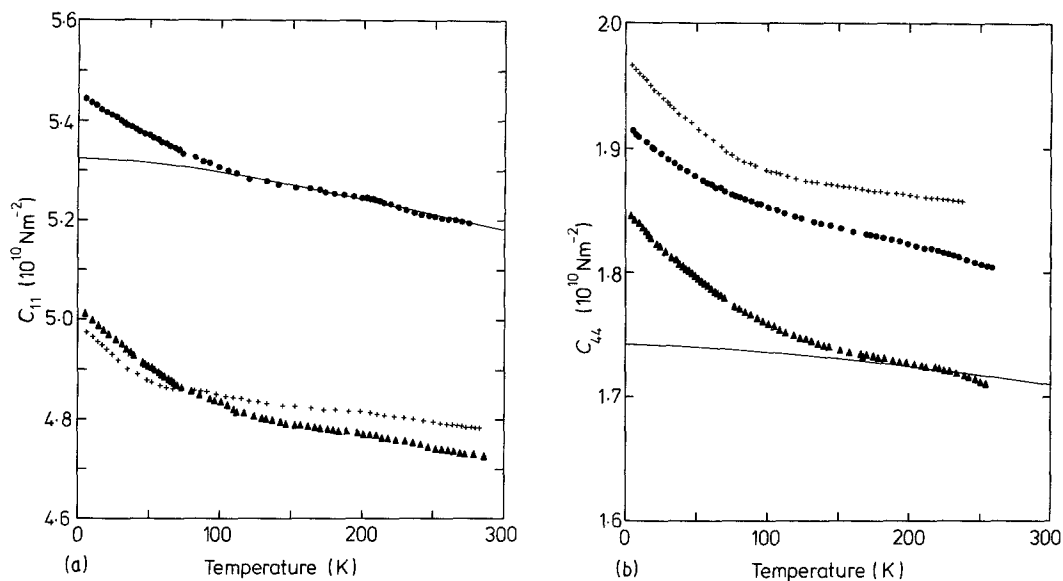


Figure 6 The temperature dependences of (a)  $C_{11}$  and (b)  $C_{44}$  for molybdenum phosphate glasses. The full lines show the temperature dependence expected for the elastic stiffnesses of the 64 mol %  $\text{MoO}_3$  glass on the basis of a quasi-harmonic Debye model for phonon anharmonicity.  $\text{MoO}_3$  content ( $\blacktriangle$ ) 37, (+) 50, ( $\bullet$ ) 64 mol %.

and

$$C_s = C_s^0 + \frac{1}{V} \left\{ -\gamma^2 (U + C_v T) - \gamma \left[ \left( \frac{\partial C_s}{\partial P} \right)_T - \frac{C_s}{3B} \right] U \right\}$$

Here the potential  $U$ , according to the Debye model, is

$$U = 3Nk\Theta \left[ 3 \left( \frac{T}{\Theta} \right)^4 \int_0^{\Theta/T} \frac{x^3 dx}{e^x - 1} \right] = 3Nk\Theta F \left( \frac{T}{\Theta} \right)$$

when  $N$  is the number of atoms in volume  $V$  and  $x = kT$ . The elastic Debye temperature (obtained from extrapolated values of the low-temperature ultrasonic wave velocity in the quasi-harmonic limit) is

$$\Theta = \left( \frac{h}{k} \right) \left( \frac{3N}{4\pi V} \right)^{1/3} \left[ \frac{1}{3} \left( \frac{1}{V_L^3} + \frac{2}{V_S^3} \right) \right]^{-1/3}$$

where  $h$  is Planck's constant. Calculations of  $C_L$  and  $C_S$  have been carried out for the 64 mol %  $\text{MoO}_3$  glass ( $\Theta = 316$  K) and are plotted in Fig. 6. The differences between the solid lines and the experimental data show that the relaxation processes produce the major contribution to the temperature dependences below 100 K of the elastic stiffnesses in these molybdenum phosphate glasses.

In region (b) (above about 130 K) we observe the normal behaviour associated with anharmonicity:  $dC_{11}/dT$  and  $d\mu/dT$  are negative and approximately constant, and are in reasonable agreement with quasi-harmonic theory (Fig. 6). The lowest magnitude of the temperature derivatives occurs at about 50 mol %

$\text{MoO}_3$ , the composition showing the smallest anharmonic effects according to the Grüneisen gammas and thermal expansion as previously discussed. Clearly the same structural and bonding factors are influencing the anharmonic effects on the pressure and temperature dependences of the elastic constants and the thermal expansion in a consistent manner.

## References

1. B. BRIDGE and N. D. PATEL, *J. Mater. Sci.* **21** (1986) 1187.
2. M. P. BRASSINGTON, W. A. LAMBSON, A. J. MILLER, G. A. SAUNDERS and Y. K. YÖGURTÇU, *Phil. Mag.* **42** (1980) 127.
3. M. P. BRASSINGTON, A. J. MILLER and G. A. SAUNDERS, *ibid.* **43** (1981) 1049.
4. E. H. BOGARDUS, *J. Appl. Phys.* **36** (1965) 2504.
5. D. S. HUGHES and J. K. KELLY, *Phys. Rev.* **92** (1953) 1145.
6. E. F. LAMBSON, G. A. SAUNDERS, B. BRIDGE and R. A. EL-MALLAWANY, *J. Non-Cryst. Solids* **69** (1984) 117.
7. M. P. BRASSINGTON, A. J. MILLER, J. PELZL and G. A. SAUNDERS, *ibid.* **44** (1981) 157.
8. N. D. PATEL, PhD thesis, University of Brunel (1982).
9. P. KIERKEGARD, K. EISTRAT and A. R. ROSENHALL, *Acta Chem. Scand.* **18** (1958) 1701.
10. R. N. THURSTON and K. BRUGGER, *Phys. Rev.* **133** (1964) A1604.
11. E. F. LAMBSON, W. A. LAMBSON, J. E. MACDONALD, M. R. J. GIBBS, G. A. SAUNDERS and D. TURNBULL, *Phys. Rev. B* **33** (1986) 2380.
12. Y. SATO and O. L. ANDERSON, *J. Phys. Chem. Solids* **41** (1980) 401.
13. F. D. MURNAGHAN, *Proc. Natn. Acad. Sci. USA* **30** (1944) 244.
14. B. BRIDGE and N. D. PATEL, *J. Mater. Sci.* in press.
15. T. N. CLAYTOR and R. J. SLADEK, *Phys. Rev.* **B18** (1978) 5842.

Received 25 July  
and accepted 22 September 1986